THE PENNSYLVANIA STATE UNIVERSITY
SCHREYER HONORS COLLEGE

DEPARTMENT OF ELECTRICAL ENGINEERING

SEGMENTATION OF ARTICULAR FEMORAL KNEE CARTILAGE USING ACTIVE SHAPE MODELS

JOHN R DURKIN
Spring 2010

A thesis
submitted in partial fulfillment
of the requirements
for a baccalaureate degree
in Computer Engineering
with honors in Electrical Engineering

Reviewed and approved* by the following:

David Miller
Associate Professor of Electrical Engineering
Thesis Supervisor

Kenneth Urish
Physician Hershey Medical Center
Thesis Co-supervisor

William Higgins
Professor Department of Electrical Engineering
Honors Adviser

* Signatures are on file in the Schreyer Honors College.

ABSTRACT

Objective: A new method for diagnosing and gauging the progression of osteoarthritis in the knee is using quantitative magnetic resonance imaging. One important step in the process of analyzing the cartilage of the knee for osteoarthritis is the segmentation of the articular femoral knee cartilage. Many conventional segmentation techniques fail because of a lack of signal contrast between the cartilage and soft tissue. The objective of this project was to use active shape models in conjunction with the geodesic active contour algorithm to produce a method for segmenting femoral articular knee cartilage from double echo steady state (DESS) magnetic resonance images.

Methods: Hand segmented femoral articular knee cartilage images from the dataset of the Osteoarthritis Initiative (OAI) were used to create an active shape model. The active shape model was then used to segment femoral articular knee cartilage from DESS images of the knee from the OAI dataset.

Results: Images segmented by the computer are compared to images segmented manually by a physician. The percent pixel-wise difference is calculated.

Keywords: osteoarthritis, knee, cartilage, segmentation, active shape models, active appearance models

TABLE OF CONTENTS

LIST OF FIGURES

LIST OF TABLES

ACKNOWLEDGEMENTS

The author would like to thank Dr. Kenneth Urish for his guidance during this project as well as Dr. David Miller and Dr. William Higgins for reading this thesis.

Chapter 1

Introduction

Knee osteoarthritis is a series disease that manifests itself in about 17.5 million people in the U.S. alone [1]. Although this is widespread disorder, especially among the geriatric population, few treatment options are available beyond simple pain management. One of the major reasons little progress has been made in the development of new treatment options is that it is difficult to diagnosis OA early and to track its early progression using plain radiography. There are, however, studies that show magnetic resonance imaging (MRI) as being a candidate for the future preferred imaging modality for early OA progression, further drug development, and risk factor identification [2].

One method of determining the healthiness of articular knee cartilage is to use T2 mapping. T2 mapping is an MR sequence that is particularly responsive to the molecular vibrations of water molecules. As cartilage breakdown occurs, the cartilage becomes more permeable to water [3]. A stronger T2 signal corresponds to an increase in the water content of cartilage and therefore cartilage damage. In addition to being able to detect the breakdown of cartilage, T2 mapping also provides a standardized quantitative method of measuring cartilage condition that is independent of the strength of the magnet in the MRI machine. Although each image is dependent on the testing environment, multiple images over time can be used in conjunction to fit to an exponential decay function whose rate of decay is independent. Therefore it provides reproducible results, regardless of the testing environment, user, machine, or magnet [4].

A problem with T2 mapping is that it provides little distinction between cartilage and some surrounding tissues and structures making it unsuitable for automated or semi-automated segmentation. Double echo steady state, or DESS imaging, does give good signal

contrast between artilcular knee cartilage and surrounding tissue, making it a suitable imaging technique for measuring cartilage volume. DESS images can be used to segment the articular cartilage to create masks defining the cartilage boundaries. The DESS images can then be registered with the T2 images, giving a boundary to the cartilage in the T2 images. Once the T2 images are segmented they can later be classified for quantitative MRI analysis.

In order to conduct a statistically significant study, multiple sets of knee cartilage must be segmented. Manual segmentation requires a qualified physician and it is time intensive. A preferred method would have an automated or semi-automated process for segmentation. Many types of image segmentation algorithms exist such as active contours (snakes), level set, and watershed, but many of these rely mostly on edge based criteria. For the segmentation of the articular femoral knee cartilage, a solely edge-based algorithm is likely to break down because of the weak boundaries at cartilage and soft tissue interfaces. Therefore, combining a model based approach and an edge detection algorithm is more desirable. One such approach was proposed by Cootes et al., and they termed their algorithm as active shape models [6].

The active shape model is a statistical model of a generic shape. The model is formed by using a training set of objects that are already segmented. Matching feature points are marked along the objects in the training set, and they are compared to find the deviation amongst the shapes. By modifying some parameters of the shape, it can be deformed to model characteristic variations of the shape. The shape is then used with a normal active contour algorithm to help constrain the region growing to only statistically likely representations of the shape.

Cootes et al. [6] used their active shape models first to segment resistors on circuit boards and later extended the algorithm to segment hands and heart ventricle walls from echocardiograms. In this paper, the algorithm is used to create an active shape model of human articular femoral knee cartilage and to segment cartilage from DESS MR Images.

1 Peterfy C. "The osteoarthritis initiative: report on the design rationale for the magnetic resonance imaging protocol for the knee". 2008.

2 Liess C, Lusse S, Karger N, Hell M and Gluer CC. "Detection of changes in cartilage water content using MRI T_2-mapping ***in vivo*** ". Osteoarthritis Cartilage. 2002 Dec; 10(12): 907-13.

3 Li X, Benjamin C, Link T, Castillo D, Blumendrantz G, Lozano J, Carballido J, Ries M, and Majumdar S. "*In vivo* T1p and T2 mapping of articular cartilage in osteoarthritis of the knee using 3T MRI. Osteoarthritis and Cartilage. 15(7): 789-797.

4 Mosher T, Smith H, Dardzinski B, Schmithorst V, and Smith M. "MR Imaging and T2 Mapping of Femoral Cartilage". American Journal of Roentgenology 2001; 177:664-669.

5 Mosher, T.J. and B.J. Dardzinski, *Cartilage MRI T2 relaxation time mapping: overview and applications.* Semin Musculoskelet Radiol, 2004. 8(4): p. 355-68.

Chapter 2

Creating the Active Shape Model

One particular solution to the identification of objects is by the creation of an active shape model, or statistical model that sufficiently describes a large proportion of the distribution of plausible shapes of a particular object. The idea was first proposed by Cootes et al in their paper [1].

Taking a sample of a large, multivariate dataset and describing its distribution with a fewer number of variables than the dataset contains is the idea behind principal component analysis, which is the statistical foundation of the active shape model. An example principal component analysis (PCA) using a bivariate dataset is given below.

Two variables X_1 and X_2 that are highly correlated can be decomposed and described by a single, new variable. The sample data used in this paper is represented in Table 2-1 and graphed in figure 2-1. The first step in principal component decomposition is to standardize the data by making the mean 0. This is accomplished by subtracting the mean from each corresponding variable, yielding a new variable:

$$X' = X - \bar{X}.$$

This transformed data set is shown in figure 2-2. The following steps use the transformed data. Next a linear combination of the data is found that best describes the distribution. Statistically this is the linear combination of X'_1 and X'_2 with the largest variance or

$$Y_1 = a_1X'_1 + a_2X'_2$$

with Y_1 having the largest variance. This is also equivalent with our bivariate data to finding a line that goes through the points with the largest variability.

The variance of Y_1 can be found using the formula

$$\delta^2(Y_1) = {a_1}^2{\delta_{x1}}^2 + {a_2}^2{\delta_{x2}}^2 + 2a_1a_2\delta_{x1}\delta_{x2}r_{x1x2}$$

Where r_{x1x2} is the correlation coefficient between each X_1 and X_2. To normalize the linear combination, a constraint is placed on transformation such that

$$1 = {a_1}^2 + {a_2}^2.$$

The solution to these equations given the sample data is

a_1 =0.18554

a_2 =0.982637.

Y_1 is called the first principal component of the dataset and the vector $<a_1,a_2>$ describes a new axis that when the data is projected onto this axis it still retains a large portion of the information. The second principal component, Y_2 describes the axes with the second most variability such that $<a_1,a_2>_{Y1}$ is orthogonal to $<a_1,a_2>_{Y2}$. In two dimensions there is only one possibility for two orthogonal axes , and therefore the second principal component for the sample data is the only orthogonal axis to Y_1

$<a_1,a_2>_{Y2}$= <0.18554, 0.982637>.

The data plotted with the new axes is shown in figure 2-3.

X1	X2
5.7	28.3
10.7	52.5
21.1	113.5
25.3	116.8
36	176.6
45.5	243

Table 2-1 Sample Data

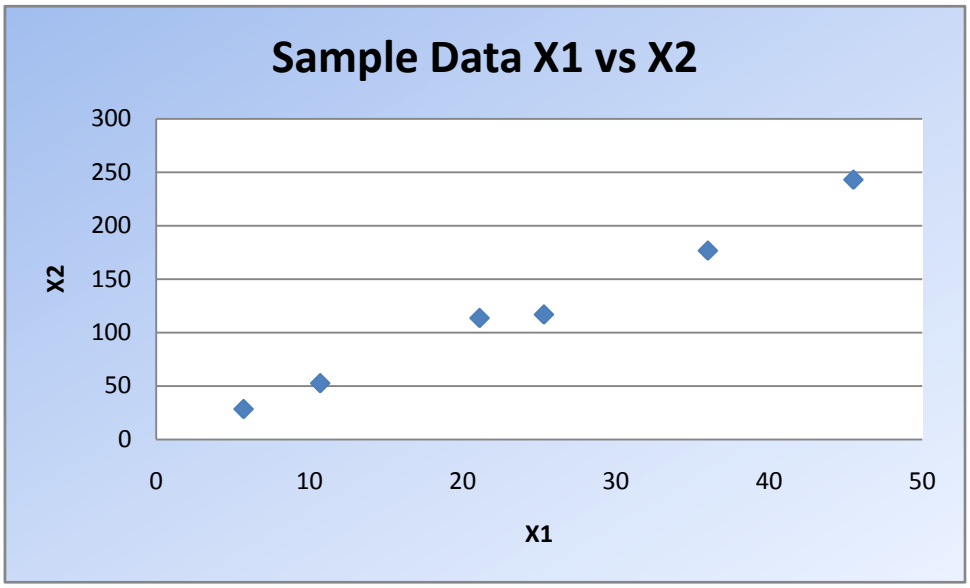

Figure 2-1 Plot of sample data, unchanged

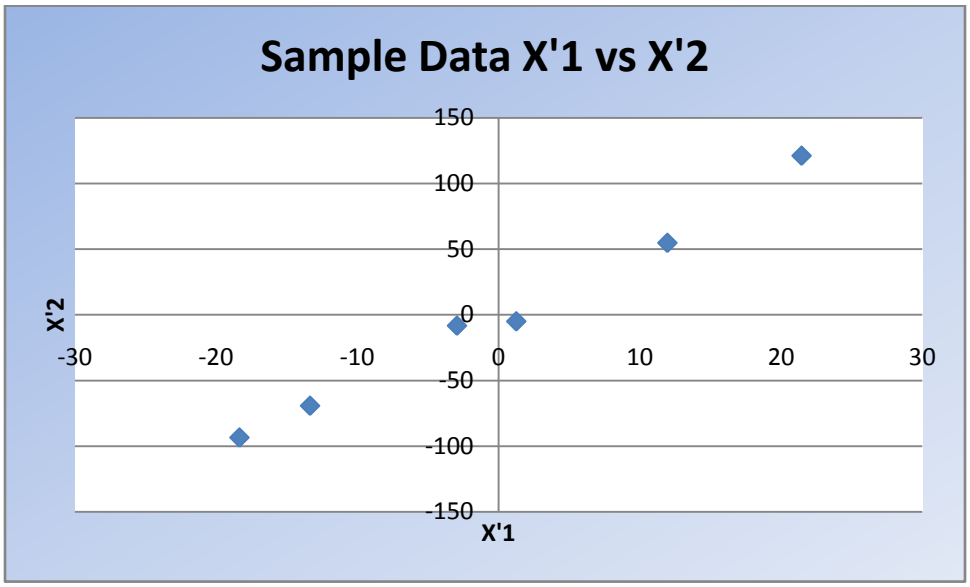

Figure 2-2 Plot of sample data transformed with a mean of 0.

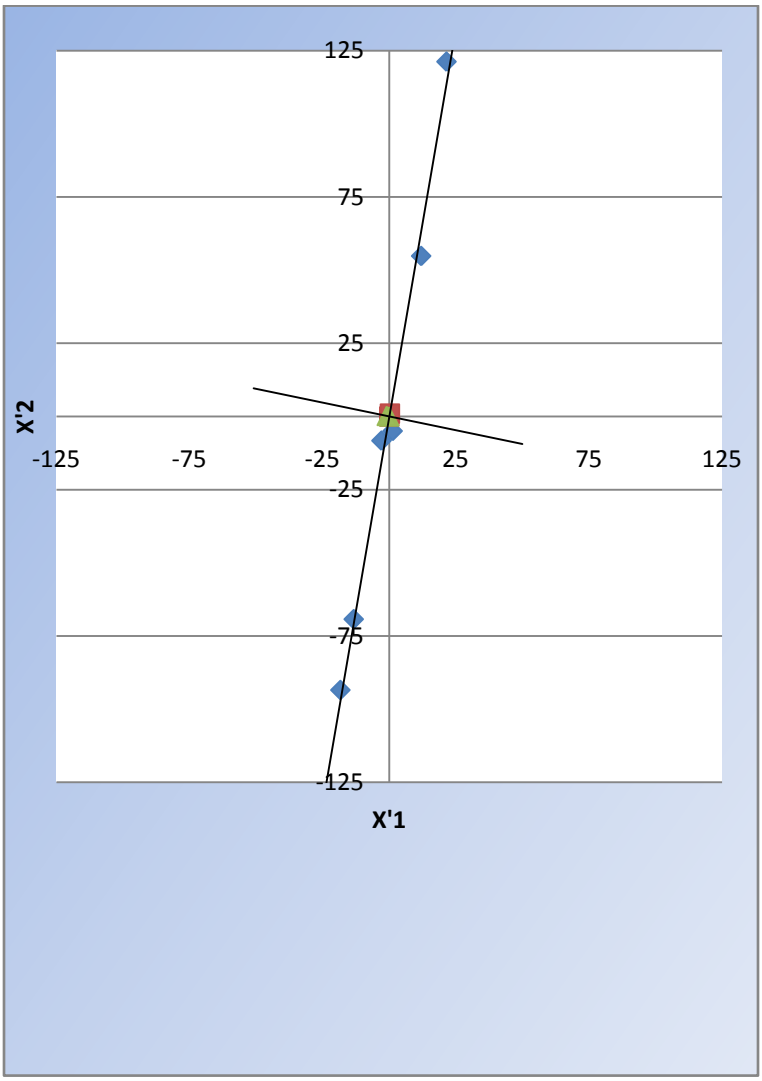

Figure 2-3. Sample data plotted with the principal component vectors.

This approach, however, is not practical for computing such vectors for more than two variables. Linear algebra and matrix manipulation software can compute principal components for N variables. To begin, a covariance matrix is formed that contains the covariance between each variable. For our two variable sample, the matrix is

$$\text{Cov} = \begin{bmatrix} Cov_{x1x1} & Cov_{x1x2} \\ Cov_{x2x1} & Cov_{x2x2} \end{bmatrix}$$

such that

$\text{Cov}_{xy} = \frac{\sum_{i=0}^{n}(x_{i-\bar{x}})(y_{i-\bar{y}})}{n-1}$.

The covariance matrix for the sample data is

$$\text{Cov} = \begin{bmatrix} 225.623 & 1182.743 \\ 1182.743 & 6266.222 \end{bmatrix}$$

Because this matrix is a square matrix, the eigenvalues and eigenvectors can be computed. For are sample data they are

$$\lambda 1 = 6489.525$$

$$EV1 = \begin{pmatrix} 0.18554 \\ 0.982637 \end{pmatrix}$$

$$\lambda 2 = 2.2995$$

$$EV2 = \begin{pmatrix} -0.98264 \\ 0.18554 \end{pmatrix}.$$

One might notice the connection between this method and the more intuitive method described earlier is the eigenvectors. These give the vectors $<a_1,a_2>_{Y1}$ and $<a_1,a_2>_{Y2}$ found previously. The eigenvalues, which were not found previously, give a number relative to the proportion of the variability of the data described by the corresponding principal component, or how much of the variability can be described by projecting the data onto the corresponding axis described by the eigenvector. 99.9646% of the variability of our sample data can be described by the first principal component. This is a useful result as the data can be reduced to one dimension with only a 0.0354% loss of information. This is shown in figure 2-4.

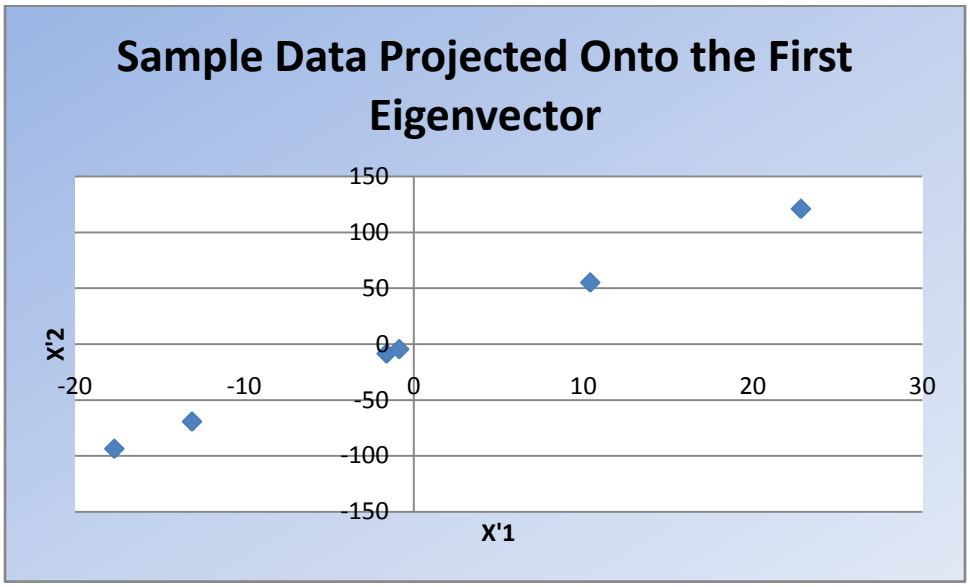

Figure 2-4 Sample data projected onto the first eigenvector.

Principal component analysis can be used to decompose the large variation in the natural shapes of femoral cartilage into a set of variables that describe the majority of the variation. To create a statistical model of femoral cartilage to be used for segmentation, a training set of previously segmented femoral cartilage images must be used. Ideally, the larger number of images in the training set, the more accurate the active shape model will be. The training images should be transformed iteratively to maximize their overlapping area. In this implementation, the N_0 iteration consisted of the training images being registered with the first training image using a similarity transform that can rotate, scale, and translate the image. After this first iteration, the mean image is computed. For the following iterations, the training images are registered to the mean image and the mean image is recomputed. This process eventually converges.

A subset of training images used to create the femoral cartilage shape model are shown in figure 2-5. From this set of transformed, registered training images, a mean model is made by taking the mean of each pixel in the training set.

$$\bar{I} = \frac{\sum_{i=1}^{N} I_i}{N}$$

The mean image for the femoral cartilage is shown in figure 2-6.

The first step of the creation of an active shape model is the identification of a set of landmarks along the outline of the shape or in this case, femoral cartilage. Landmarks are a set of points (x,y) in the training images that describe the outline of the shapes. Each image should have the same number of landmarks and they should correspond to the same location on the general shape. An automatic landmark detection system is made by finding the pixels that lie on the shape edges of the mean image. Each pixel must be a certain distance, or tolerance away or else they converge into a single landmark.

Each of these landmarks is then tracked on each training image. The N landmarks are represented by variables X_0, X_1, …, X_{n-1}. Each training image is subtracted from the mean image so that the data is normalized for principal component analysis.

$$I'_i = I_i - \bar{I}$$

The nxn covariance matrix is then computed. The size of the covariance matrix is equal to N^2 where N is the number of landmarks.

$$\text{Cov} = \begin{pmatrix} Cov_{x0x0} & \cdots & Cov_{x0xn-1} \\ \vdots & \ddots & \vdots \\ Cov_{xn-1x0} & \cdots & Cov_{xn-1xn-1} \end{pmatrix}$$

After principal component analysis is performed, by finding the determinate of the covariance matrix, we have a set of eigenvalues and corresponding eigenvectors. All of the training images can be reconstructed by combining a linear combination of the eigenvectors and the mean image. An ample number of eigenvectors are chosen such that the sum of their eigenvalues yield a large portion of variation. The eigenvalues for each principal component of the femoral cartilage shape model are given in table 2-2. The first principle component contains

the majority of the variation at about 70%. Using the first four principle components, about 96% of the variation of the knee cartilage can be represented.

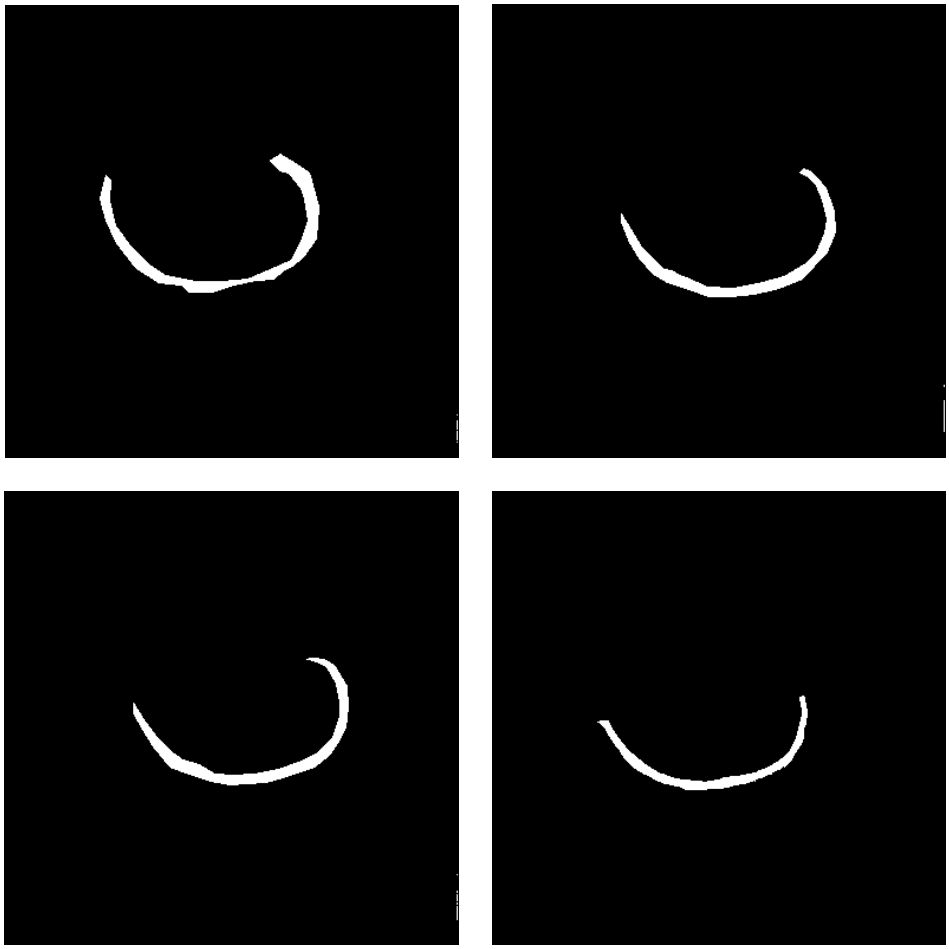

Figure 2-5 Subsample of the training images used

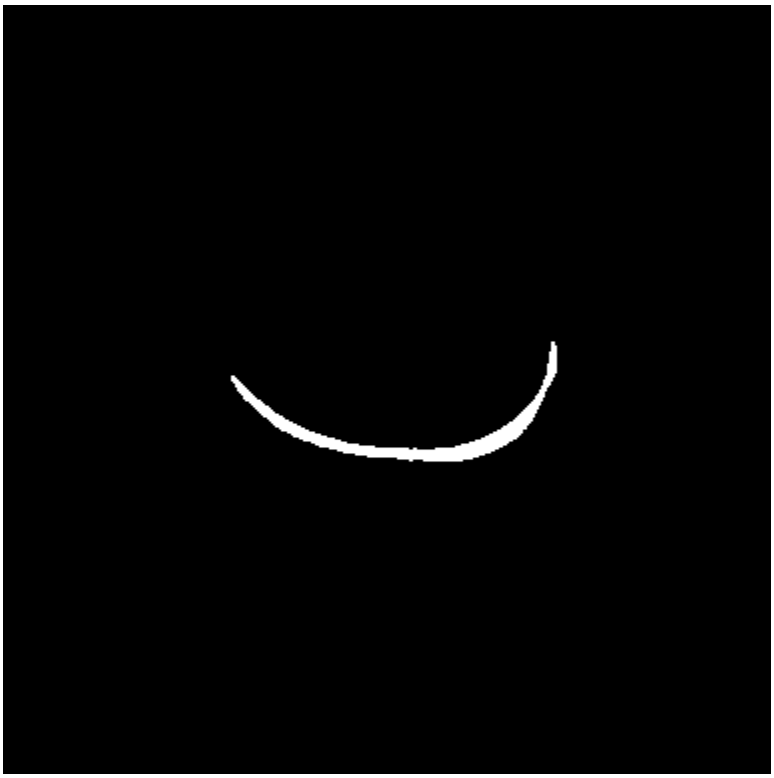

Figure 2-6 mean image for femoral articular knee cartilage.

λ in order of decreasing magnitude	$\frac{\lambda}{\sum \lambda}$
8.13E+06	54%
4.34E+06	29%
1.76E+06	12%
4.23E+05	3%
1.32E+05	1%
9.03E+04	1%
7.59E+04	1%
4.81E+04	0%
3.89E+04	0%
3.42E+04	0%
2.22E+04	0%
1.57E+04	0%
1.36E+04	0%
1.01E+04	0%
8.51E+03	0%
6.48E+03	0%
5.84E+03	0%
5.02E+03	0%

Table 2-2 Eigenvalues for each principal component and the percent of the sum of all eigenvalues.

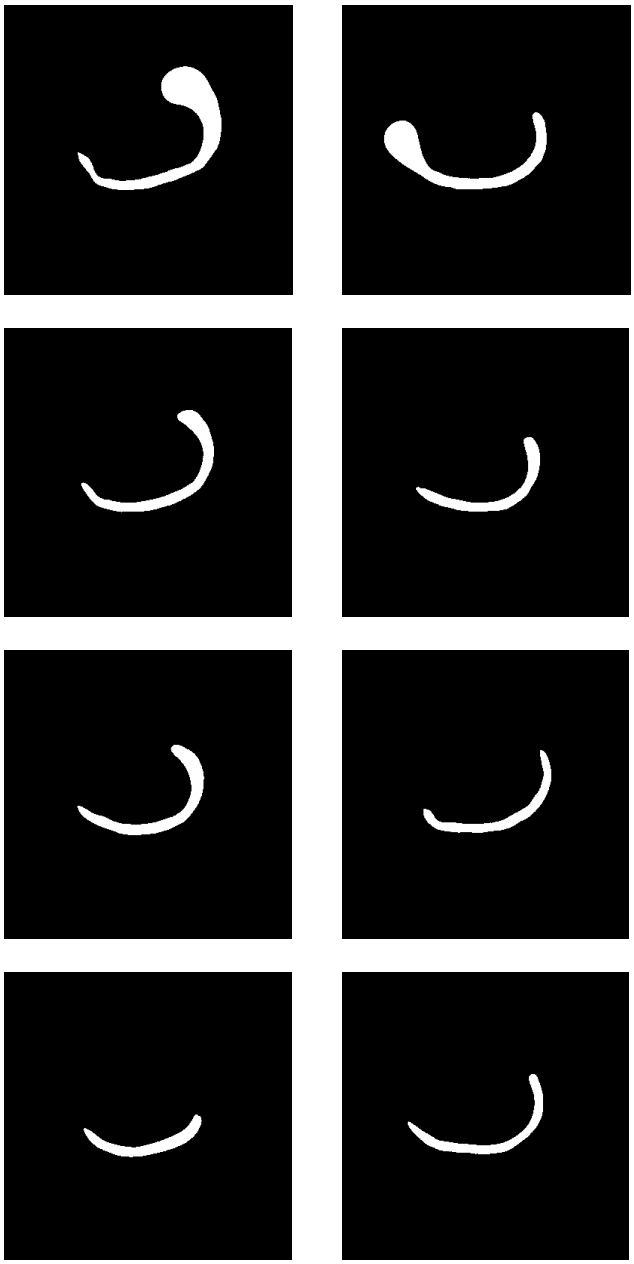

Figure 2-7. $\bar{X} \mp 2\sigma$ for λ1-λ4 from top to bottom

Figure 2-7shows the first four principle components influence on the mean shape. The first principle component controls the shift in the mass of the cartilage from the left to the right

side. The influence of the other components is less easily describable but can be seen.

1 Cootes T, Taylor C, Cooper D, and Graham J. “Active Shape Models—Their Training and Application”. Computer Vision and Image Understanding Vol. 61, No. 1, January, pp. 38-59, 1995.

2 Flury, Bernhard and Riedwyl, Hans. *Multivariate Statistics a practical approach.* New York, NY: Chapman and Hall 1988.

3 Smith, Lindsay. “A tutorial on Principal Component Analysis”. 26 February, 2002. <http://www.cs.otago.ac.nz/cosc453/student_tutorials/principal_components.pdf>

Chapter 3

Segmentation Using Active Shape Models

Many algorithms for segmentation, including the one presented in this thesis, are based off of level sets. Level sets are used to describe the evolution of a contour (2D images) or surface (3D images) by introducing an extra dimension (usually time). The contour equation $\varphi(X)$ thus becomes $\varphi(X, t)$ and the current position of the contour can be found by extracting the output at t = 0. This representation of evolving contours is preferred because it tends to handle the situations such as splitting and merging of multiple contours implicitly. The level set of a contour can be represented by a 3D volume. A 2D slice along the time scale at t = r, gives the contour at time r. Figure 3-1 shows this and how the convergence and divergence of multiple contours is handled.

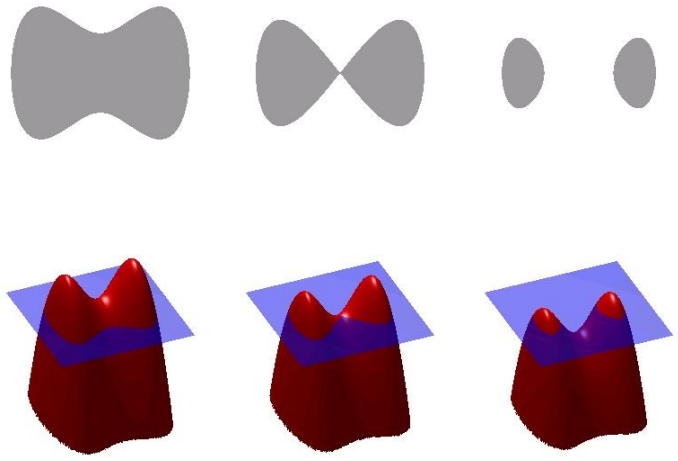

Figure 3-1. 2 dimensional slices at $t=t_0$ of the surface describing the level set give the contour at time $t=t_0$. (original image released to the public from http://www.rpi.edu/~chens/Research.html).

As a typical paradigm for contour control, a user initializes one or more contours by placing seed points from which the contours will evolve. The contour then grows, governed by a

differential equation, and is attracted to image features such as high gradient image edges. The general equation is as follows:

$$\frac{d}{dt}\varphi = -\alpha A(x) * \nabla\varphi - \beta P(x)|\nabla\varphi| + \gamma Z(x)k|\nabla\varphi|$$

Where A(x) is a term for the advection, which attracts the level set to object boundaries, P(x) is a propagation term, which controls the expansion of the contours, and Z(x)k controls the influence of the mean curvature of the contour. α, β, and γ are weights that correspond to the advection, propagation, and curvature terms. Simply increasing or decreasing the weights can increase or decrease the influence of each term. $\varphi(x)$ should converge when the contour is on the shape.

An active shape model can be used to introduce a new term into the differential equation. This term is $\varepsilon[\varphi^*(x) - \varphi(x)]$. $\varphi^*(x)$ is equal to

$$\varphi^*(x) = \mu + \sum_k a_k u_k \ ,$$

which represents the estimated best fit shape using the mean shape (μ) and each principal component (u_k) along with the corresponding weights (a_k). Therefore $[\varphi^*(x) - \varphi(x)]$ represents the amount of the best fit shape that lies outside the contour. It causes the contour to be attracted to the best fit shape. To control the influence of this term among the curvature, advection, and propagation, a weight ε is introduced. With this new term the final differential equation describing the contour's evolution becomes

$$\frac{d}{dt}\varphi = -\alpha A(x) * \nabla\varphi - \beta P(x)|\nabla\varphi| + \gamma Z(x)k|\nabla\varphi| + \varepsilon[\varphi^*(x) - \varphi(x)]$$

Much of the algorithm relies on being able to define image edges and separate them from uniform regions. The image used to define image edges is known as an edge potential image. This image should have high values (close to 1) where the image intensity is constant and the

contour should propagate quickly and low values (close to 0) when near an image edge and 0 at an image edge to slow down and stop the propagating contour.

The first step is to smooth the image. There are many options for smoothing such as Gaussian blur, median filtering, alpha trimmed, etc, each with their own benefits and downfalls. In this application anisotropic diffusion filter was used. Anisotropic diffusion based off of Perona et al [1]. It is an iterative nonlinear smoothing filter that approximates an image smoothed by convolution with a Gaussian. Each iteration, t, is approximately equivalent to convolution with a Gaussian with a larger sigma or

$$I(x, y, t) = I_o * G(x, y, t).$$

To prevent the filter from smoothing across edges and to encourage it to smooth along constant regions, a conduction coefficient, c(x,y,t), is introduced. c(x,y,t) is computed from a function $g(||\nabla I||)$ where $||\nabla I||$ is the normalization of the image gradient. $g(||\nabla I||)$ should map large gradients, which are presumably image edges, close to zero so no smoothing occurs, and small gradients, which are presumably constant regions, close to one so smoothing is greatest. Some common functions used are

$$g(||\nabla I||) = e^{-\left(\frac{||\nabla I||}{k}\right)^2}$$

and

$$g(||\nabla I||) = \frac{1}{1 + \left(\frac{||\nabla \mathrm{I}||}{k}\right)^2}$$

Each successive iteration is found by the equation

$$I(x, y, t) = c(x, y, t)\Delta I(x, y, t-1) + \nabla c \nabla I(x, y, t-1)$$

with the initial condition

$$I(x, y, 0) = I_0(x, y).$$

Figure 3-2 shows an unfiltered DESS MRI of a knee. Figure 3-3 shows the knee after running anisotropic diffusion. As one can see, the image is smoothed with little to no distortion along boundaries.

Figure 3-2 Original DESS MRI of Knee

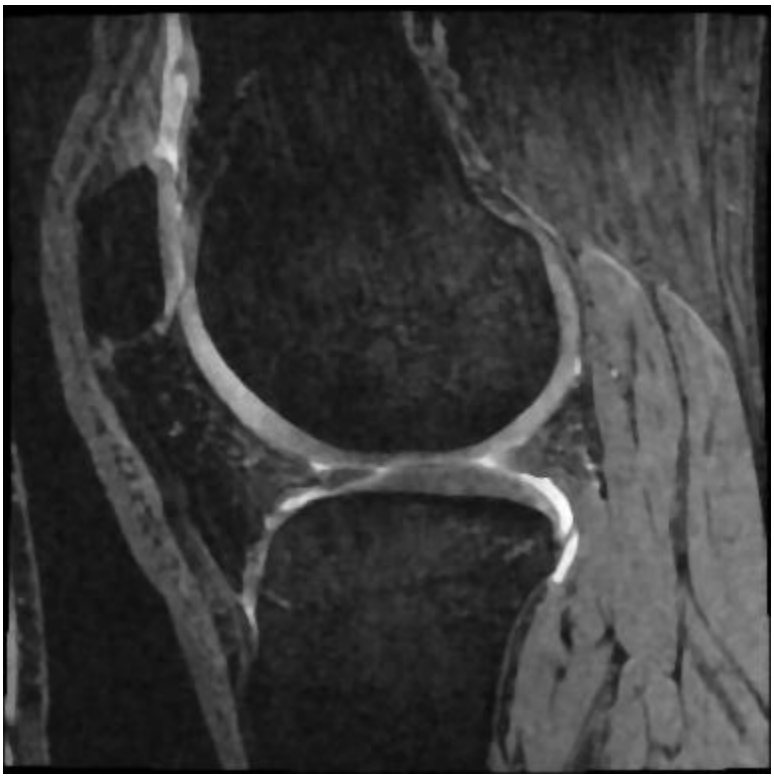

Figure 3-3 Knee image after applying anisotropic diffusion filter.

The next step in obtaining the edge potential image is to find the edges. Using the smoothed image, the edges are found by passing this image through a finite difference filter, which approximates the derivative along the x and y axis. The output of this filter is shown in figure 3-4. For the edge potential map we want areas of high gradient to be near 0 and areas of low gradient to be 1. There are a couple of methods to execute this transformation. The first and simplest is to use the bounded reciprocal function.

$$I'(x,y) = \frac{1}{1 + I(x,y)}$$

This function, however, does not give much flexibility. Another method known as the sigmoid filter offers more flexibility with two parameters: α and β.

$$I'(x,y) = \frac{1}{1 + e^{-\frac{I(x,y)-\beta}{\alpha}}}$$

β defines the center of the intensities of the original image. Intensities above β should be mapped to 0 and intensities below β should be mapped to 1. α defines the steepness of the transformation. The larger α is in magnitude, the more the transformation will become a ramp, while the smaller α is in magnitude, the more the transformation will resemble a step function. α will be negative in our implementation in order to accomplish mapping small values to large values and large to small. The output of the sigmoid filter can be seen in figure 3-5.

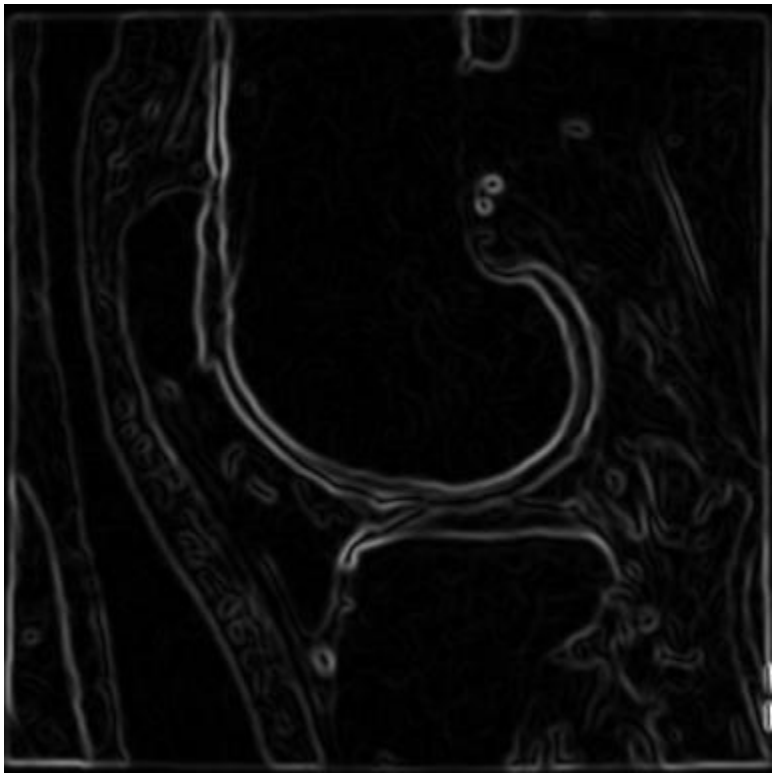

Figure 3-4. Output of the image gradient filter

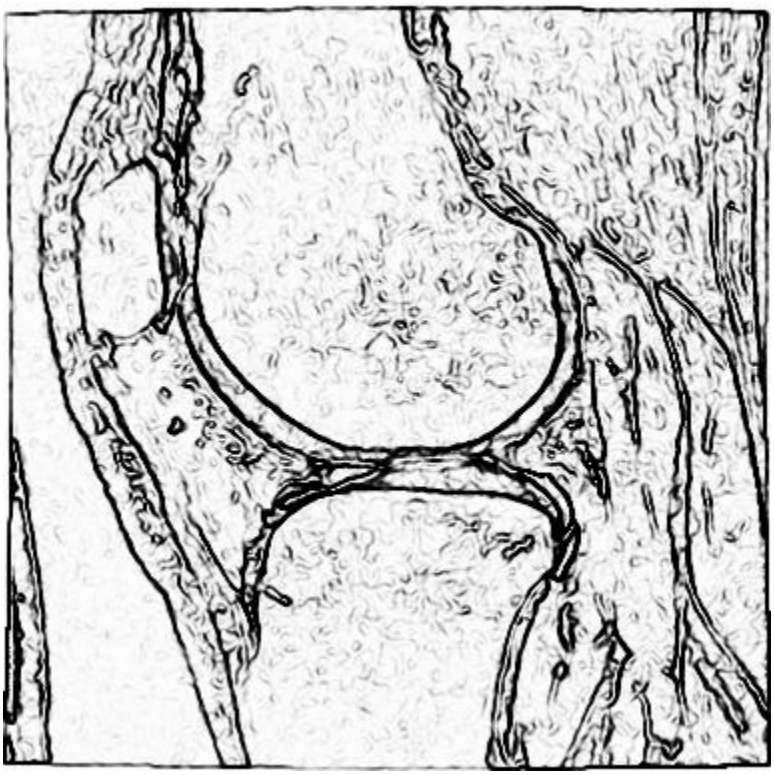

Figure 3-5 Output of Sigmoid Filter

In addition to this edge potential image, we must also create an initial level set. The initial level set comes from the contours surrounding the initial seed points. The level set is then just a signed distance function relative to the seed points. An initial level set after placing four seed points along the medial condyle of the articular knee cartilage is given in figure 3-6. A segmentation result is given in figure 3-7.

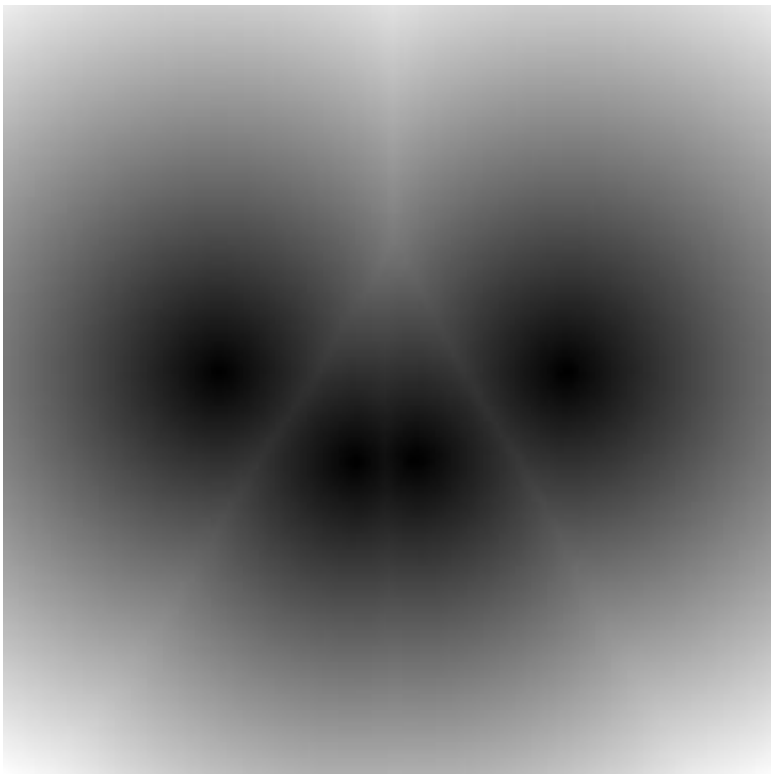

Figure 3-6 Initial level set.

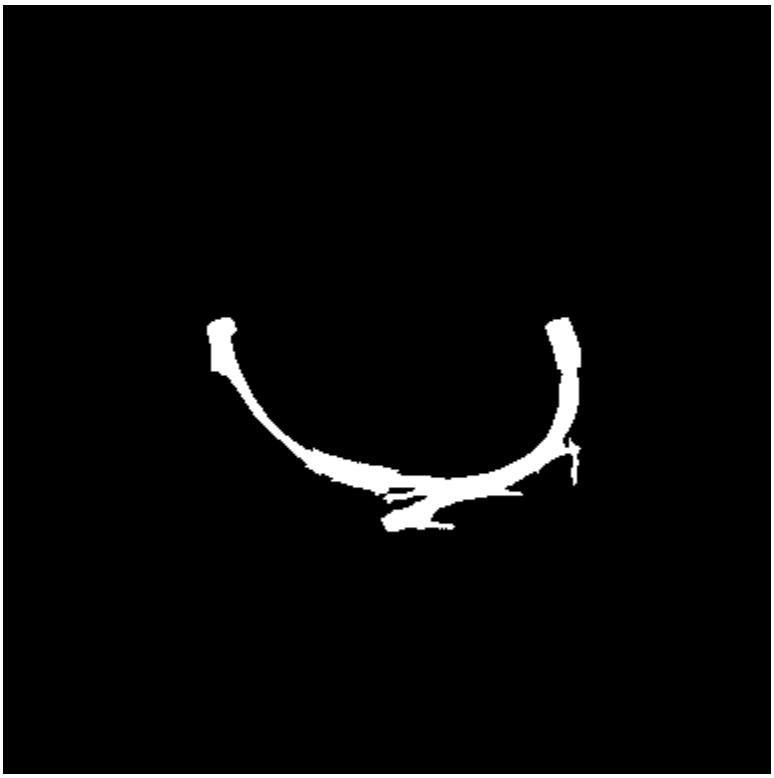

Figure 3-7. Segmentation result.

1 Perona P and Malkik J. “Scale-Space and Edge Detection Using Anisotropic Diffusion”. IEEE Transactions of Pattern Analysis and Machine Intelligence. Vol. 12. No. 7, July 1990.

2 Sethian, J.A. “Level Set Methods: An Act of Violance. Cambridge University Press, 1996.

3 Leventon M, Grimson W, and Faugeras O. “Statistical shape influence in geodesic active contours. In *Proc. IEEE Conference on Computer Vision and Pattern Recognition.* Volumne 1. Pp. 316-323, 2000.

4 Caselles V, Kimmel R, and Sapiro G. “Geodesic Active Contours”. International Journal of Computer Vision. 22(1), 61-79(1997).

5 Ibanez L, Schroeder W, Ng L, Cates J. The ITK Software Guide Second Edition. November 21, 2005.

Chapter 4

Validation of the Segmentation

In order to validate the accuracy of the segmentation, the program-segmented images were compared with the same DESS MR images manually segmented by a physician. To visually compare the manually segmented and program segmented cartilage images three regions were defined: one region representing the area segmented by both methods, another area segmented only by the manual segmentation, and the area falsely interpreted by the program as the articular femoral knee cartilage. To objectively determine the accuracy of the segmentation, the percent difference of the segmentations was computed using the following formula

$$\%Difference = \frac{P_m + P_c - 2(P_m \cap P_c)}{P_m}$$

Where P_m are the pixels inside the manually segmented image and P_c are the pixels inside the computer segmented image. Figure 4-1 shows the results for a few segmentations. The segmented areas are shown in color and laid over the original DESS MR image. The percent differences are also shown for each image.

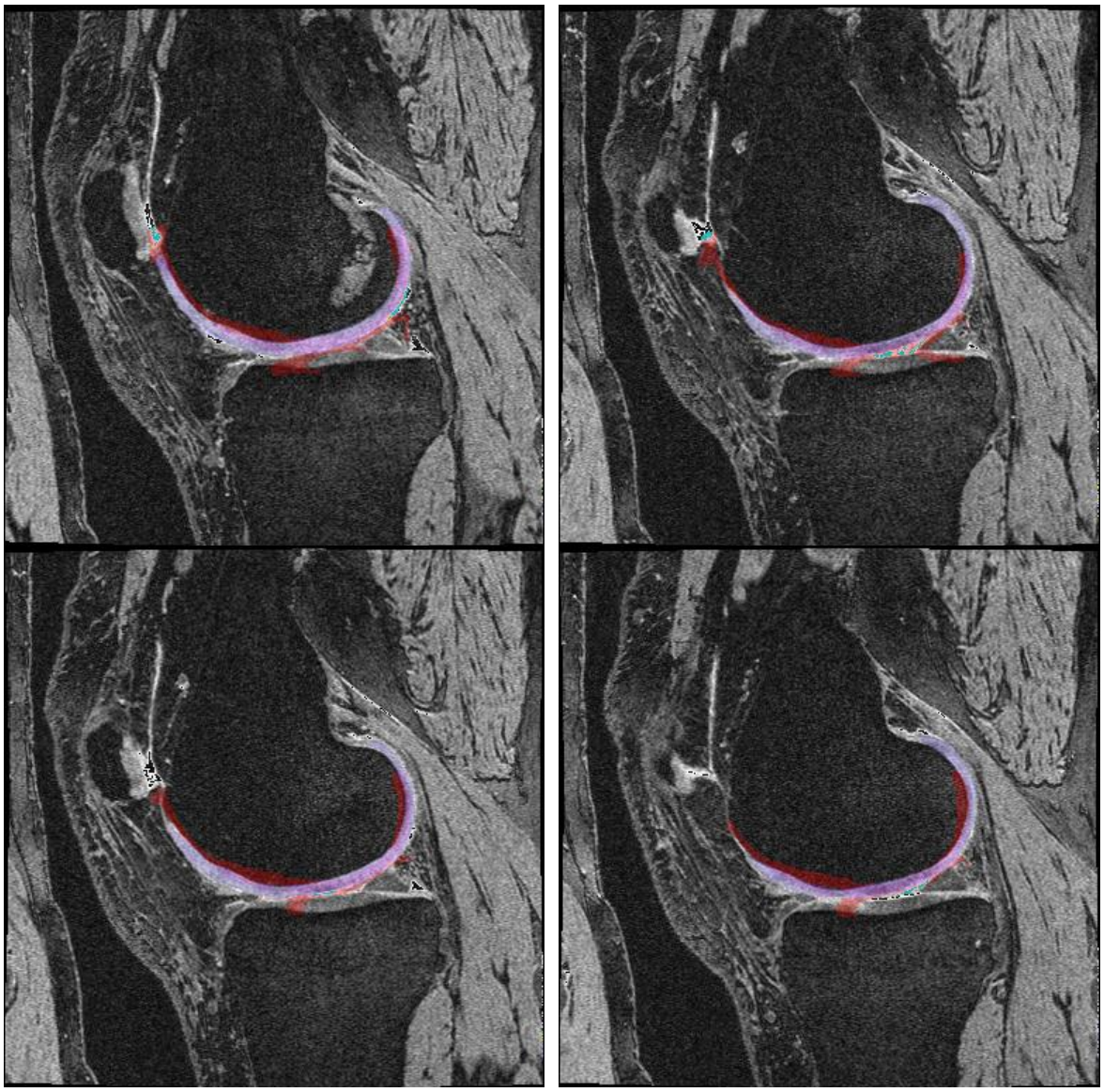

Figure 4-1. Results of the computer segmentation compared with manual segmentation. Magenta regions are pixels inside the computer segmented cartilage and not the manual. Blue refers to regions inside the manual segmented cartilage and not the computer segmented cartilage. Purple regions are included in both segmentations. The percent differences are: top-left: 23%, top-right: 28%, bottom-left: 19%, bottom-right: 26%.

Chapter 5

Conclusion

In the diagnosis and study of the progress of osteoarthritis of the knee, magnetic resonance imaging is becoming an important tool. An imperative step in the quantitative analysis of osteoarthritis of the knee is the segmentation of the articular femoral knee cartilage from the MR image. This task is not easily accomplishable using standard segmentation techniques that rely solely on gradient based algorithm because of the lack of distinction between the cartilage and soft tissues at interfaces. Using active shape models as an additional term in the classical level sets equation prevents leakage across these indistinct boundaries, and allows a more accurate segmentation of the cartilage.

This paper presented the theory behind active shape models and their use in level set segmentation and gave its implementation on segmenting articular femoral knee cartilage from DESS MR images of the knee. In addition, the segmentation results were validated using a pixelwise percent difference of the computer segmented images and their corresponded manually segmented images by a qualified physician. Although this implementation of the algorithm gives moderate results, there is room for improvement. The most noticeable breakdown of the segmentation is the leaking into the articular tibial cartilage. This mostly arises from the extremely weak boundary between the femoral and tibial cartilage. A more accurate shape model and a higher weight applied to its term in the level set equation should minimize such leakage and be included in a future implementation.

Another breakdown of this implementation comes from the large variation in the shapes of the sagital slices of femoral articular knee cartilage. It is difficult representing all such slices in a single two dimensional model. A lot of work has been done lately on the creation and use of

three dimensional active shape models[1-3]. In future work, this algorithm should be extended to work in 3 dimensions, to create a better represented shape model.

1 Rousson M, Paragios N, and Deriche R. “Implicit Active Shape Models for 3D Segmentation in MR Imaging.

2 Fripp J, Warfield S, Crozier S, and Ourselin S. “Automatic Segmentation of the Knee Bones using 3D active Shape Models”. 18th International Conference on Pattern Recognition Volumne 1.

3 Solloway S, Taylor C, Hutchinson C, and Waterton J. “Quantification of articular cartilage from MR images using active shape models”. Computer Vision—EECV 1996. Pp. 400-411.

CURRICULUM VITAE

BIOGRAPHICAL

Name: John R. Durkin

Address: 255 E Beaver Ave Apt # 611
State College, PA 16801

Phone: (215) 538-7443

Permanent Address: 2280 Spinnerstown Rd
Quakertown, PA 18951

Cell Phone: (267) 664-0044

Birth Date: Dec 28, 1987

Citizenship: USA

E-Mail Address: jrd5084@psu.edu

EDUCATION and TRAINING

UNDERGRADUATE

2006-2010 The Pennsylvania State University — BS, Computer Engineering
Honors Thesis: "Visualization and Segmentation of Femoral Knee Cartilage"
Advisor: David Miller, PhD
Co-advisor: Kenneth Urish, MD PhD
The Schreyer Honors College
State College, PA

Spring 2008 VENUSA — Minor, Spanish
Mérida, Venezuela

APPOINTMENTS and POSITIONS

2008-2010 Kenneth Urish, MD PhD
The Penn State Hershey Medical Center
Hershey, PA
"Medical image analysis: segmentation and registration of knee cartilage on MR images."

2009-2010 Richard Tutwiler, PhD
The Pennsylvania State University Applied Research Lab
State College, PA
"Development of a visualization interface, storage methods, and filter methods for flash LIDAR data."

Fall 2009 Thomas Barnett, MS
Weldon
Columbus, OH
"Development of a high-powered adjustable focus LED light for emergency vehicles."

Summer 2008 Grandview Hospital Department of Emergency Medicine
Sellersville, PA
Emergency Technician

PUBLICATIONS

Under Preparation

Urish KL, Williams A., **Durkin J.**, Chu C. (2009). Registration and Semi-automated Segmentation of Femoral Knee Articular Cartilage

2010 The ITK Software Guide. The Insight Toolkit. The National Institute of Health, The National Library of Medicine. Creation of an Active Shape Model for Use With Geodesic Active Contours Segmentation With Shape Guidance.

HONORS

2008 Lockheed Martin Excellence in Engineering Award Recipient
2007 Whole World Scholarship Recipient

2006 Lutron Scholarship Recipient

TEACHING

2009-2010 Math, Chemistry, Physics, Programming, and Biology Tutor. PSU Know How. State College, PA.

2007 Calculus and Linear Algebra Grader and Proctor. Department of Mathematics, The Pennsylvania State University, State College, PA.

SERVICE

Global Connections

2008-2010 Help foreign exchange students and immigrants with English and American Culture

The Pennsylvania State University Dance Marathon

2006-2010 Raised money for Four Diamonds Fund to help offset the costs of pediatric cancer for families of patients through an organization called Atlas Thon

TECHNICAL and OTHER SKILLS

Foreign Languages

Spanish read, write, speak at Advanced level

Programming Skills

C, C++, VTK, ITK, OpenCV, Qt, Java, Matlab, VHDL, Derby Database